Free-Standing $LiNi_{0.5}Mn_{1.5}O_4$/Carbon Nanofiber Network Film as Lightweight and High-Power Cathode for Lithium Ion Batteries

Xin Fang,[†] Mingyuan Ge,[†] Jiepeng Rong,[†] and Chongwu Zhou[†,‡,*]

[†]Mork Family Department of Chemical Engineering and Materials Science and [‡]Ming Hsieh Department of Electrical Engineering, University of Southern California, Los Angeles, California 90089, United States

ABSTRACT Lightweight and high-power $LiNi_{0.5}Mn_{1.5}O_4$/carbon nanofiber (CNF) network electrodes are developed as a high-voltage cathode for lithium ion batteries. The $LiNi_{0.5}Mn_{1.5}O_4$/CNF network electrodes are free-standing and can be used as a cathode without using any binder, carbon black, or metal current collector, and hence the total weight of the electrode is highly reduced while keeping the same areal loading of active materials. Compared with conventional electrodes, the $LiNi_{0.5}Mn_{1.5}O_4$/CNF network electrodes can yield up to 55% reduction in total weight and 2.2 times enhancement in the weight percentage of active material in the whole electrode. Moreover, the $LiNi_{0.5}Mn_{1.5}O_4$/carbon nanofiber (CNF) network electrodes showed excellent current rate capability in the large-current test up to 20C (1C = 140 mAh/g), when the conventional electrodes showed almost no capacity at the same condition. Further analysis of polarization resistance confirmed the favorable conductivity from the CNF network compared with the conventional electrode structure. By reducing the weight, increasing the working voltage, and improving the large-current rate capability simultaneously, the $LiNi_{0.5}Mn_{1.5}O_4$/CNF electrode structure can highly enhance the energy/power density of lithium ion batteries and thus holds great potential to be used with ultrathin, ultralight electronic devices as well as electric vehicles and hybrid electric vehicles.

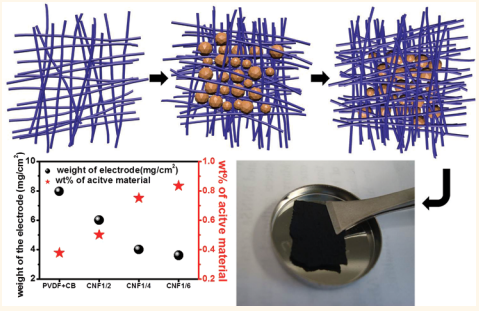

KEYWORDS: lithium ion batteries · high-voltage cathode · $LiNi_{0.5}Mn_{1.5}O_4$ · carbon nanofiber · free-standing · high-power

The lithium ion battery field has experienced continuous progress since Sony commercialized the first lithium ion battery in the early 1990s. Nowadays, lithium ion batteries are widely used as power sources and energy storage devices in our daily life, especially in the market of portable electronics. Despite the great success of lithium ion batteries up to now, higher demand has been raised with the emergence of new-generation electronic products, such as ultrathin and ultralight devices. In addition, the development of electric vehicles, hybrid electric vehicles, and plug-in hybrid electric vehicles also requires further enhancement of battery performance. Innovation in battery technology is thus highly desired to fulfill the ever-increasing demand of higher power/energy density, better rate capability, and longer cycle life.[1−3]

As the energy density of the batteries can be calculated from $\int_0^Q V(q)\,dq/wt$, improving the energy density of batteries has to be accomplished in three ways: increasing voltage, increasing capacity, or reducing weight.[4] Using a high-voltage cathode has been well recognized as an effective way to increase the voltage of lithium ion batteries, since the working voltage of the anode has almost reached the working potential of lithium metal.[5] Among the high-voltage cathode materials, $LiNi_{0.5}Mn_{1.5}O_4$ is considered as one of the most promising candidates due to the double redox couples, Ni^{2+}/Ni^{3+} and Ni^{3+}/Ni^{4+}, where a relatively high capacity can be obtained.[6,7] With a high working voltage of 4.7 V and theoretical capacity of 146.7 mAh/g, $LiNi_{0.5}Mn_{1.5}O_4$ can provide 20% and 30% higher energy density than traditional cathode materials $LiCoO_2$ and $LiFePO_4$, respectively.[8−10] To further

* Address correspondence to chongwuz@usc.edu.

Received for review February 10, 2014 and accepted April 7, 2014.

Published online 10.1021/nn500814v

enhance the energy density, reducing the weight of the batteries can be an important and essential strategy.

Recently, new designs of battery electrodes have been reported, which replace or even eliminate the use of binders or current collectors in conventional battery electrode structure.[11−20] These designs have stimulated a new trend of developing high-energy-density lithium ion batteries through lightweight electrodes. However, to the best of our knowledge, there has been no report on further improving the energy density of lithium ion batteries with a coeffect of a high-voltage cathode together with novel design of electrode structure.

In this study, we report the first free-standing $LiNi_{0.5}Mn_{1.5}O_4$/carbon nanofiber (CNF) electrode without using any other conductive additives, polymer binders, or metal current collectors. Through this approach, we are able to reduce the weight and increase the working voltage of the electrodes simultaneously, hence resulting in a complementary enhancement of the energy/power density of the electrode. The electrodes consist of $LiNi_{0.5}Mn_{1.5}O_4$ particles synthesized *via* a highly scalable solid-state reaction method and CNFs that are mass produced and commercially available already. The $LiNi_{0.5}Mn_{1.5}O_4$ particles are distributed in a free-standing CNF network, which provides direct access to the electrolyte and also facilitates electron transfer.

Through our design of electrode structure, the following benefits can be achieved: (1) the total weight of the electrodes is highly reduced, since the CNFs can act as binder, conductive additive, and current collector simultaneously, and no other electrochemically inactive additives will be needed in the electrodes; (2) the conductivity of the electrodes is greatly enhanced due to the good conductivity of the CNFs compared with the traditional binders, which are usually insulating; (3) the continuous and porous CNF network facilitates electrolyte infiltration in addition to electron transfer, and in this way the $LiNi_{0.5}Mn_{1.5}O_4$ particles can access Li ions more efficiently; (4) our active material $LiNi_{0.5}Mn_{1.5}O_4$ provides high working voltage, while the CNF network renders the electrode lightweight, and hence the energy density is enhanced by a combined effect of increasing voltage and reducing weight simultaneously. In the meanwhile, the capacity is not compromised at all since $LiNi_{0.5}Mn_{1.5}O_4$ offers a similar capacity compared with other traditional cathode materials such as $LiCoO_2$.

RESULTS AND DISCUSSION

Our free-standing $LiNi_{0.5}Mn_{1.5}O_4$/CNF network electrodes were fabricated through vacuum filtration. To ensure that the particles are trapped inside the CNF network instead of easily falling out from the surface, the surface was covered by an extra thin layer of CNF network. The process is shown as a schematic diagram in Figure 1a−c and also described in detail in the

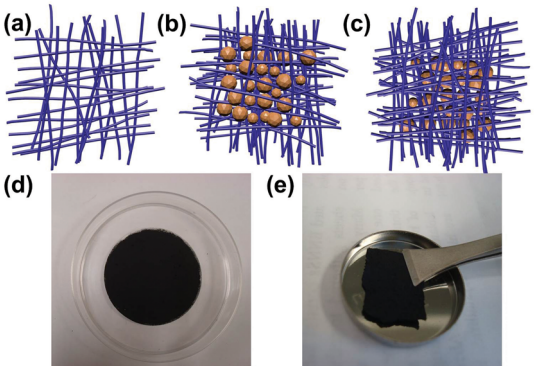

Figure 1. Schematics and photos of $LiNi_{0.5}Mn_{1.5}O_4$/carbon nanofiber (CNF) network electrodes. (a−c) Schematic showing the fabrication process: bottom CNF thin layer (a), main part of $LiNi_{0.5}Mn_{1.5}O_4$ and CNF added (b), and final coverage with CNF thin layer (c). (d) Photo of the $LiNi_{0.5}Mn_{1.5}O_4$/CNF network after filtration. (e) Photo of the free-standing $LiNi_{0.5}Mn_{1.5}O_4$/CNF network electrode before assembling into a battery.

Experimental Section. Briefly, a small amount of CNFs was first filtrated to get a thin CNF layer on the bottom, as shown in Figure 1a, and then the main part of the electrode, the $LiNi_{0.5}Mn_{1.5}O_4$/CNF mixture, was filtrated on top (shown in Figure 1b). After that, a final thin layer of CNF network was added to cover the top surface, as shown in Figure 1c. The weight ratios of CNFs and $LiNi_{0.5}Mn_{1.5}O_4$ particles were 1:1, 1:3, and 1:5, denoted by CNF1/2, CNF1/4, and CNF1/6, respectively. A digital image of the $LiNi_{0.5}Mn_{1.5}O_4$/CNF network after filtration is shown in Figure 1d. The network can be easily peeled off from the filtration paper after drying and cut into small electrodes to assemble coin cells. Figure 1e shows the digital image of the free-standing electrode that is cut into coin cell size and ready for assembling. Traditionally, metal foils are used in batteries as current collectors, which work as a conductive support for electron transport. As both the active cathode material and carbon black are particles, polymer binders such as poly(vinylidene fluoride) (PVDF) are needed to connect the particles to the metal current collector. In our new design of the $LiNi_{0.5}Mn_{1.5}O_4$/CNF network electrodes, since electrodes are free-standing and the CNF network is conductive, it is not necessary to attach the $LiNi_{0.5}Mn_{1.5}O_4$/CNF network onto a current collector. The CNFs are entangled and form a network configuration, so the $LiNi_{0.5}Mn_{1.5}O_4$ particles can be trapped inside and connected by the CNF network; thus no binder is needed. Also, as the CNFs are conductive, conductive additives such as carbon black are not needed either. As a result, the total weight of the electrode is highly reduced.

The whole electrode is made of $LiNi_{0.5}Mn_{1.5}O_4$ particles and CNFs exclusively. $LiNi_{0.5}Mn_{1.5}O_4$ can be synthesized *via* a variety of methods, such as co-precipitation,[21] solid-state reaction,[22,23] sol−gel method,[24] thermal polymerization,[25] molten salt method,[26] and so on. Among

these methods, co-precipitation and solid-state reaction are adopted by industry since they are most scalable and compatible with industrial processing. In our work, we used a modified solid-state reaction to prepare $LiNi_{0.5}Mn_{1.5}O_4$, thus having the potential for large-scale applications. Hollow CNFs used in this study are mass-produced and purchased from Pyrograp Products Inc. Transmission electron microscope (TEM) images of the CNFs are shown in Figure 2a and b. Figure 2a reflects the hollow nature of the CNFs, and Figure 2b clearly shows the detailed structure of the walls. The outer diameter of the CNFs is over 100 nm, and the inner diameter is 50−60 nm. The layered structure of the walls can be clearly seen in the high-resolution transmission electron microscope (HRTEM) image of Figure 2b. The graphitic nature of the CNFs is beneficial in enhancing the conductivity of the electrodes, thus leading to the superior performance under large current density and fast charge/discharge. A scanning electron microscope (SEM) image of the surface of the free-standing $LiNi_{0.5}Mn_{1.5}O_4$/CNF network electrodes is shown in Figure 2c. It is obvious that the surface is covered by a CNF network and no $LiNi_{0.5}Mn_{1.5}O_4$ particles can be seen. The CNFs are over 100 μm in length and are entangled with each other. This approach allows us to fully utilize $LiNi_{0.5}Mn_{1.5}O_4$ particles without losing them during battery assembling or cycling. Figure 2d, e, and f reveal the interior of the $LiNi_{0.5}Mn_{1.5}O_4$/CNF composite electrodes, where CNFs take 1/2, 1/4, and 1/6 of the total weight, respectively. It is evident from these SEM images that the $LiNi_{0.5}Mn_{1.5}O_4$ particles are evenly distributed in the CNF network. In this way, the CNF network can provide an electron pathway to the $LiNi_{0.5}Mn_{1.5}O_4$ particles and enhance the conductivity of the whole electrode. In addition, the network is strong enough to accommodate a large loading of $LiNi_{0.5}Mn_{1.5}O_4$ particles inside, as in the case of CNF1/6 samples, the CNF network can hold $LiNi_{0.5}Mn_{1.5}O_4$ particles that are five times the weight of CNFs.

Figure 3 presents the battery test results from free-standing $LiNi_{0.5}Mn_{1.5}O_4$/CNF network electrodes with all three compositions. As a control, conventional electrodes were also tested in the same condition. After 100 cycles at a regular current rate of C/2, the capacity retention of CNF1/2, CNF1/4, CNF1/6, and a conventional electrode is 98.3%, 95.7%, 94.2%, and 93.9%, respectively. Results from extended cycles of CNF1/2, CNF1/4, and CNF1/6 are shown in Figure 3b, which have demonstrated the cycling stability for up to 500 cycles. Although the specific capacity of conventional electrodes is higher than CNF1/6, it is obvious from Figure 3c that all free-standing $LiNi_{0.5}Mn_{1.5}O_4$/CNF network electrodes showed much superior performance under large current rates. It is noteworthy that at a current rate as large as 20C the conventional electrodes showed almost no capacity, while the $LiNi_{0.5}Mn_{1.5}O_4$/CNF network electrodes can still deliver 99.3 mAh/g (CNF1/2), 69.0 mAh/g (CNF1/4), and 65.3 mAh/g (CNF1/6). It is evident from the results here that the CNF network provides a much better conductivity to the whole electrode than

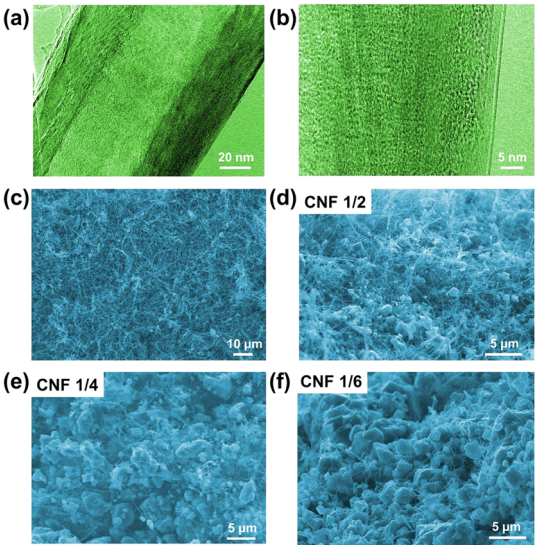

Figure 2. (a) TEM and (b) HRTEM image of CNF; (c) SEM image of the surface of the $LiNi_{0.5}Mn_{1.5}O_4$/CNF network; (d−f) SEM images of the inside of the $LiNi_{0.5}Mn_{1.5}O_4$/CNF network for compositions of CNF1/2 (d), CNF1/4 (e), and CNF1/6 (f).

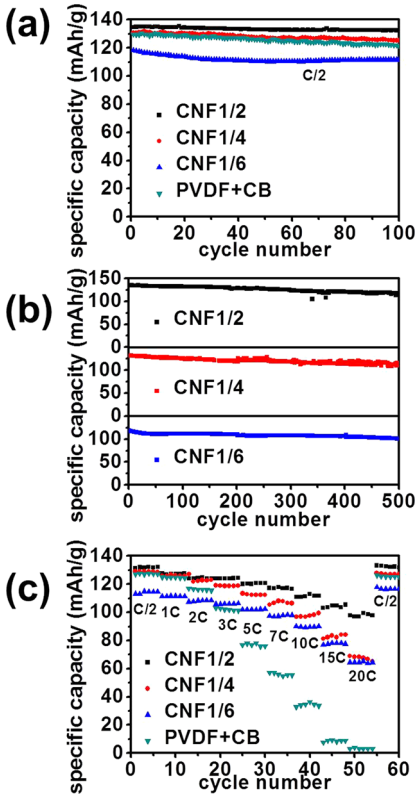

Figure 3. (a) Comparison of cycling performance of $LiNi_{0.5}Mn_{1.5}O_4$/CNF network electrodes and conventional electrodes at C/2 (1C = 140 mAh/g); (b) extended cycling results from $LiNi_{0.5}Mn_{1.5}O_4$/CNF network electrodes for up to 500 cycles at C/2; (c) comparison of discharge capacity of $LiNi_{0.5}Mn_{1.5}O_4$/CNF network electrodes and conventional electrodes from C/2 to 20C. Charging rate was kept at C/2.

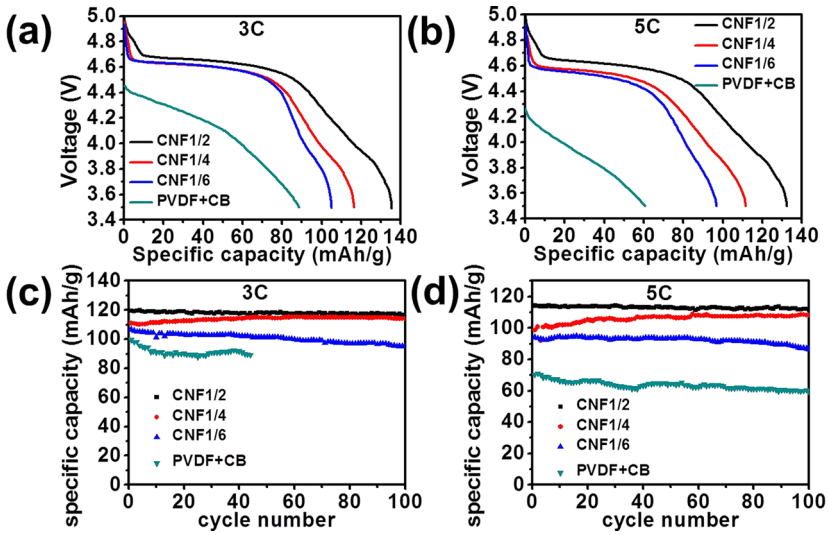

Figure 4. Discharge curves of $LiNi_{0.5}Mn_{1.5}O_4$/CNF network electrodes and conventional electrodes at 3C (a) and 5C (b). Cycling performance of $LiNi_{0.5}Mn_{1.5}O_4$/CNF network electrodes and conventional electrodes at 3C (c) and 5C (d). Charging rate was also 3C or 5C, correspondingly.

conventional PVDF and carbon black. The remarkable performance demonstrated the advantages of employing a CNF network in the electrode structure. We note here that a pure CNF network without $LiNi_{0.5}Mn_{1.5}O_4$ was also tested in the voltage window of 3.5−5 V with Li metal as counter electrode. All other conditions were kept the same as the battery tests for $LiNi_{0.5}Mn_{1.5}O_4$/CNF network electrodes and conventional electrodes. The result is shown in Figure S1 (Supporting Information). From Figure S1 it is clear that CNFs can provide only around 20 mAh/g capacity in the voltage window of 3.5−5 V. In order to eliminate this effect and make a fair comparison among all electrodes, we have deducted the capacity from CNFs when calculating the specific capacities.

To examine the cyclability of the free-standing $LiNi_{0.5}Mn_{1.5}O_4$/CNF network electrodes at large current rate, the batteries were tested at 3C and 5C for 100 cycles continuously. The results are shown in Figure 4. Figure 4a and b represent the discharge curves at 3C and 5C, respectively. The CNF1/2 electrodes maintained a high voltage plateau at 4.67 V at 3C, while the CNF1/4 and CNF1/6 electrodes provided 4.62 V. At 5C, CNF1/2 electrodes kept a working voltage of 4.64 V, while the voltage of CNF1/4 and CNF1/6 electrodes slightly decreased to 4.58 and 4.56 V, respectively. Compared to the free-standing $LiNi_{0.5}Mn_{1.5}O_4$/CNF network electrodes, it is obvious that conventional electrodes cannot maintain the working voltage during large current cycling, and hence the energy and power provided by these batteries have been severely reduced. The cyclability results in Figure 4c and d have proved that the free-standing $LiNi_{0.5}Mn_{1.5}O_4$/CNF network electrodes can sustain large current charge/discharge continuously without compromising cycle life. However, it is not meaningful to discuss the capacity of conventional electrodes since the high voltage plateau cannot be reserved. The comparison here has revealed the advantages of free-standing $LiNi_{0.5}Mn_{1.5}O_4$/CNF network electrodes: not only is the total weight of the electrode reduced, but also the current rate capability and retention are enhanced, both leading to significant improvement in energy/power density of the batteries.

It has been reported that polarization behavior plays an important role in the rate capability of the batteries.[27,28] To further study the effect of a CNF network on the rate capability of the electrodes, polarization resistance (R_p) was calculated based on methods presented in the literature.[27,28] The batteries were discharged at different current rates to obtain discharge profiles shown in Figure 5. It is clear that the $LiNi_{0.5}Mn_{1.5}O_4$/CNF network electrodes maintained higher capacity and voltage than conventional electrodes at large current densities. Comparing with $LiNi_{0.5}Mn_{1.5}O_4$/CNF network electrodes, the conventional electrodes almost cannot deliver any capacity at the high voltage range under current densities larger than 5C. Further analysis was performed following refs 27 and 28 to determine the polarization resistance, which is defined as the slope of $E(I_m) = f(I_m)$, where E is the potential, I_m is the mass current, and $f(I_m)$ is the correlation between potential and mass current. With the curves at different discharge rates, the voltage *vs* mass current profile from different depths of discharge (DOD) can be obtained, as shown in Figure 6. For example, the black curve in Figure 6a was obtained by extracting the voltage values corresponding to 20% of DOD from curves in Figure 5a with different current rates. According to the relation $R_p = V/I$, polarization resistance R_p can be extracted from the slope of voltage *vs* mass current curves. After doing linear fit for each of the curves in Figure 6, R_p values at different DOD were

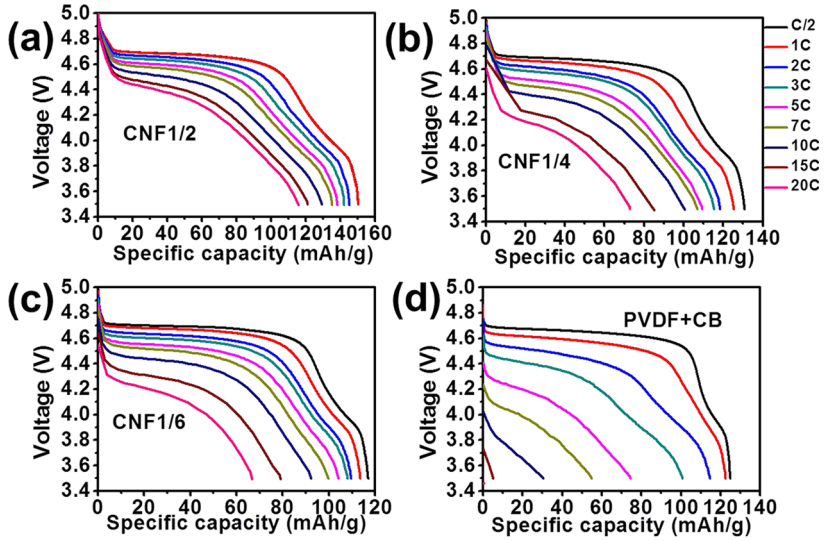

Figure 5. Discharge profiles of CNF1/2 (a), CNF1/4 (b), CNF1/6 (c), and conventional electrodes (d) from C/2 to 20 C.

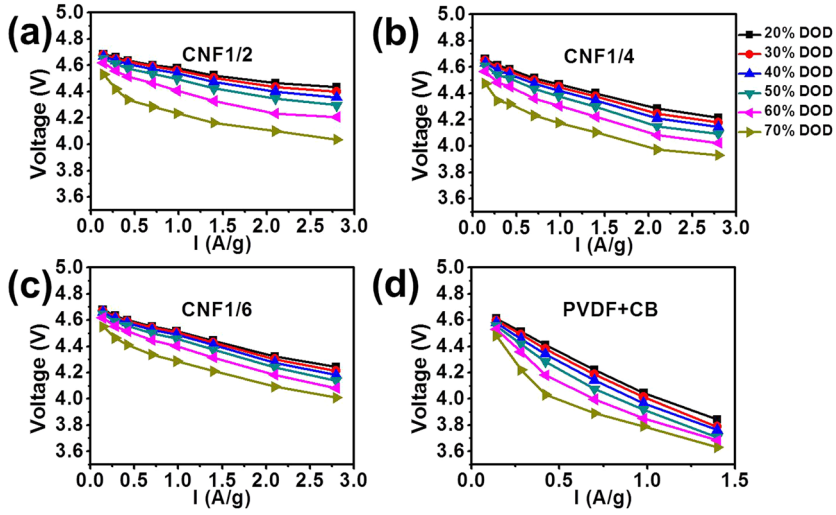

Figure 6. Voltage *vs* mass current profiles of CNF1/2 (a), CNF1/4 (b), CNF1/6 (c), and conventional electrodes (d) from 20% to 70% depth of discharge.

obtained and plotted in Figure 7. It should be clarified that the R_p values here represent the polarization resistance of the whole battery instead of the cathode only. However, since the Li anode metal, separator, electrolyte, and battery case are identical in all batteries, the difference in R_p can be an index of the difference between free-standing $LiNi_{0.5}Mn_{1.5}O_4$/CNF network electrodes and conventional electrodes.

It is obvious from Figure 7 that conventional electrodes bear much larger polarization resistance than the $LiNi_{0.5}Mn_{1.5}O_4$/CNF network electrodes. Among the $LiNi_{0.5}Mn_{1.5}O_4$/CNF network electrodes, CNF1/2 showed the lowest R_p values owing to the largest CNF content. The R_p values from CNF1/4 and CNF1/6 turned out to be close to each other. We believe this is because the difference between CNF contents of 25% and 16.7% is not sufficiently significant to distinguish from the voltage plateau of Ni^{2+}/Ni^{3+} and Ni^{3+}/Ni^{4+} redox couples. Instead, the larger capacity of CNF1/4 came from the domain below the working voltage of Ni^{2+}/Ni^{3+} and Ni^{3+}/Ni^{4+} redox couples to the cutoff voltage of 3.5 V. By judging the discharge profiles together with the R_p values, we believe a decrease of CNF content from 25% to 16.7% will not affect the energy/power delivered from the high-voltage region. However, if the full capacity needs to be utilized, a slightly higher CNF content such as 25% would be beneficial in releasing the energy beyond the high-voltage region. All $LiNi_{0.5}Mn_{1.5}O_4$/CNF network electrodes showed much smaller R_p values than the conventional electrodes, indicating the favorable conductivity enhancement from the CNF network. Nevertheless, we note that the charge transfer mechanism between the CNF and $LiNi_{0.5}Mn_{1.5}O_4$ is not well understood and deserves further study.

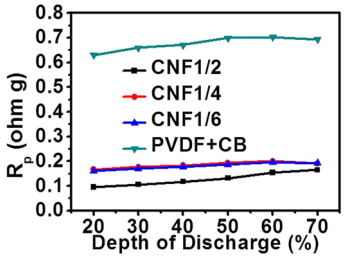

Figure 7. Comparison of polarization resistance of batteries with $LiNi_{0.5}Mn_{1.5}O_4$/CNF network electrodes and conventional electrodes.

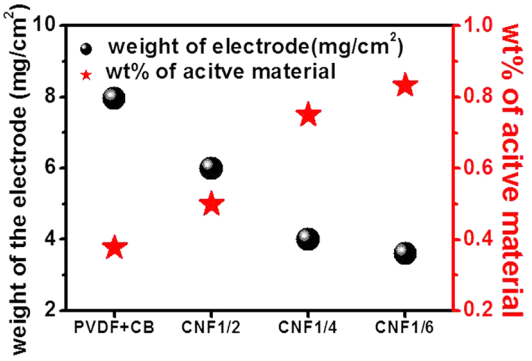

Figure 8. Comparison of $LiNi_{0.5}Mn_{1.5}O_4$/CNF network electrodes and conventional electrodes in terms of weight of the electrodes and weight percentage of active material in the electrodes. The calculation was based on an active material loading of 3 mg/cm^2.

In addition to the polarization study, we also compared the total weight of the different electrodes as well as the active material weight percentage (wt %) in the electrodes, shown in Figure 8. Compared with conventional electrodes, the $LiNi_{0.5}Mn_{1.5}O_4$/CNF network electrodes can yield up to 55% reduction in total weight and 2.2 times enhancement in the wt % of active material in the whole electrode. Since these properties strongly affect the gravimetric energy/power density of the batteries, the reduced weight and enhanced wt % of active material will lead to considerable improvements in lightweight and high-power lithium ion batteries.

CONCLUSION

In summary, we have developed a free-standing $LiNi_{0.5}Mn_{1.5}O_4$/CNF network electrode as a high-voltage cathode for lithium ion batteries. This new design of electrode structure can reduce the total weight in addition to improving the working voltage of the electrode, thus resulting in a further enhancement of energy density. The free-standing $LiNi_{0.5}Mn_{1.5}O_4$/CNF network electrodes showed excellent performance in a fast charge/discharge cycling test, which demonstrated their capability in sustaining large current during battery operation. Moreover, the remarkable current rate capability also enables us to develop high-power lithium ion batteries with the free-standing $LiNi_{0.5}Mn_{1.5}O_4$/CNF network electrodes. With highly scalable production of both $LiNi_{0.5}Mn_{1.5}O_4$ and CNFs, the new method has great potential to promote the development of lightweight and high-power lithium ion batteries for ultrathin and ultralight electronic devices and even electric vehicles in the future.

EXPERIMENTAL SECTION

Materials Preparation. A solid-state reaction was employed to prepare $LiNi_{0.5}Mn_{1.5}O_4$ particles. Nickel acetate ($Ni(Ac)_2 \cdot 4H_2O$) and manganese acetate ($Mn(Ac)_2 \cdot 4H_2O$) were first mixed at a molar ratio of Ni:Mn = 1:3 and hand-milled in a mortar. The mixture was then heated to 500 °C with a heating rate of 3 °C/min. After 5 h heat treatment, lithium acetate ($LiAc \cdot 2H_2O$) was added to the mixture with a molar ratio of Li:Ni:Mn = 2.1:1:3 (5% excess lithium acetate was added in order to make up for the volatilization of Li during calcination), and the mixture was heated to 500 °C for 5 h again. After that, the mixture was milled and sintered at 950 °C for 10 h followed by annealing at 700 °C for 10 h.

CNFs were obtained from Pyrograf Products Inc. (Pyrograf-III, Carbon Nanofiber, PR-24-XT-HHT, batch information: PS 1392 BOX 5 HT 183). The CNFs were produced *via* chemical vapor deposition and heat-treated afterward to graphitize the carbon overcoat on the surface. According to the manufacturer,[29] the CNFs were highly conductive after heat treatment. The average diameter was 100 nm and the surface area was 35−45 m^2/g. The CNFs were treated with nitric acid and sulfuric acid (3:1, v/v) at 90 °C overnight in order to break up bundles. The CNFs were then washed with DI water and collected by filtration.

Free-standing $LiNi_{0.5}Mn_{1.5}O_4$/CNF network electrodes were prepared through vacuum filtration. The weight ratios of CNFs and $LiNi_{0.5}Mn_{1.5}O_4$ particles were 1:1, 1:3, and 1:5, denoted by CNF1/2, CNF1/4, and CNF1/6, respectively. During filtration, a small amount of CNFs was first added to the filtration system to obtain a thin layer of CNF network at the bottom. Then the $LiNi_{0.5}Mn_{1.5}O_4$/CNF mixture was added to form the main part of the free-standing composite film. On top of the mixture, another CNF thin layer was added again. This way, both the top and bottom surfaces were cover by a CNF network in order to prevent $LiNi_{0.5}Mn_{1.5}O_4$ particles from falling out. The weight ratios here take into account all the CNFs used in the electrodes, including CNFs used for surfaces and inside the electrodes. According to a previous study on CNF-containing composites,[30,31] the percolation threshold is around or below 3 wt %. Therefore, our CNF1/2, CNF1/4, and CNF1/6 samples are all above the percolation threshold, and the CNF network should provide good electric conduction.

Electrochemical Measurements. CR 2032 coin cells were assembled with Li metal as counter electrodes. A 1.2 M solution of $LiPF_6$ in ethylene carbonate and dimethyl carbonate (3:7) was used as electrolyte. The batteries were cycled in the voltage range 3.5−5 V. The free-standing $LiNi_{0.5}Mn_{1.5}O_4$/CNF network electrodes were used directly as a cathode in batteries. As a control, conventional electrodes were also prepared by slurry-casting on an Al current collector with the weight ratio $LiNi_{0.5}Mn_{1.5}O_4$:poly(vinylidene fluoride):carbon black = 8:1:1. To make a fair comparison, the active material loading of all electrodes was maintained between 2 and 3 mg/cm^2.

Conflict of Interest: The authors declare no competing financial interest.

Acknowledgment. We acknowledge financial support from Joint KACST/California Center of Excellence.

Supporting Information Available: The specific capacity of a pure CNF network without $LiNi_{0.5}Mn_{1.5}O_4$ was also tested in the

voltage window 3.5−5 V with Li metal as the counter electrode. This material is available free of charge *via* the Internet at http://pubs.acs.org.

REFERENCES AND NOTES

1. Tarascon, J. M.; Armand, M. Issues and Challenges Facing Rechargeable Lithium Batteries. *Nature* **2001**, *414*, 359–367.
2. Armand, M.; Tarascon, J. M. Building Better Batteries. *Nature* **2008**, *451*, 652–657.
3. Kim, T. H.; Park, J. S.; Chang, S. K.; Choi, S.; Ryu, J. H.; Song, H. K. The Current Move of Lithium Ion Batteries towards the Next Phase. *Adv. Energy Mater.* **2012**, *2*, 860–872.
4. Goodenough, J. B.; Kim, Y. Challenges for Rechargeable Batteries. *J. Power Sources* **2011**, *196*, 6688–6694.
5. Goodenough, J. B.; Kim, Y. Challenges for Rechargeable Li Batteries. *Chem. Mater.* **2010**, *22*, 587–603.
6. Amine, K.; Tukamoto, H.; Yasuda, H.; Fujita, Y. Preparation and Electrochemical Investigation of $LiMn_2$-XMe_xO_4 (Me: Ni, Fe, and x = 0.5, 1) Cathode Materials for Secondary Lithium Batteries. *J. Power Sources* **1997**, *68*, 604–608.
7. Zhong, Q. M.; Bonakdarpour, A.; Zhang, M. J.; Gao, Y.; Dahn, J. R. Synthesis and Electrochemistry of $LiNi_xMn_2$-XO_4. *J. Electrochem. Soc.* **1997**, *144*, 205–213.
8. Liu, D.; Zhu, W.; Trottier, J.; Gagnon, C.; Barray, F.; Guerfi, A.; Mauger, A.; Groult, H.; Julien, C. M.; Goodenough, J. B.; Zaghi, K. Spinel Materials for High-Voltage Cathodes in Li-Ion Batteries. *RSC Adv.* **2014**, *4*, 154–167.
9. Fang, X.; Ge, M. Y.; Rong, J. P.; Zhou, C. W. Graphene-Oxide-Coated $LiNi_{0.5}Mn_{1.5}O_4$ as High Voltage Cathode for Lithium Ion Batteries with High Energy Density and Long Cycle Life. *J. Mater. Chem. A* **2013**, *1*, 4083–4088.
10. Fang, X.; Ge, M.; Rong, J.; Che, Y.; Aroonyadet, N.; Wang, X.; Liu, Y.; Zhang, A.; Zhou, C. Ultrathin Surface Modification by Atomic Layer Deposition on High Voltage Cathode $LiNi_{0.5}Mn_{1.5}O_4$ for Lithium Ion Batteries. *Energy Technol.* **2014**, *2*, 159–165.
11. Jia, X. L.; Yan, C. Z.; Chen, Z.; Wang, R. R.; Zhang, Q.; Guo, L.; Wei, F.; Lu, Y. F. Direct Growth of Flexible $LiMn_2O_4$/CNT Lithium-Ion Cathodes. *Chem. Commun.* **2011**, *47*, 9669–9671.
12. Jia, X. L.; Chen, Z.; Suwarnasarn, A.; Rice, L.; Wang, X. L.; Sohn, H.; Zhang, Q.; Wu, B. M.; Wei, F.; Lu, Y. F. High-Performance Flexible Lithium-Ion Electrodes Based on Robust Network Architecture. *Energy Environ. Sci.* **2012**, *5*, 6845–6849.
13. Luo, S.; Wang, K.; Wang, J. P.; Jiang, K. L.; Li, Q. Q.; Fan, S. S. Binder-Free $LiCoO_2$/Carbon Nanotube Cathodes for High-Performance Lithium Ion Batteries. *Adv. Mater.* **2012**, *24*, 2294–2298.
14. Wang, K.; Luo, S.; Wu, Y.; He, X. F.; Zhao, F.; Wang, J. P.; Jiang, K. L.; Fan, S. S. Super-Aligned Carbon Nanotube Films as Current Collectors for Lightweight and Flexible Lithium Ion Batteries. *Adv. Funct. Mater.* **2013**, *23*, 846–853.
15. Zhu, H. L.; Jia, Z.; Chen, Y. C.; Weadock, N.; Wan, J. Y.; Vaaland, O.; Han, X. G.; Li, T.; Hu, L. B. Tin Anode for Sodium-Ion Batteries Using Natural Wood Fiber as a Mechanical Buffer and Electrolyte Reservoir. *Nano Lett.* **2013**, *13*, 3093–3100.
16. Chen, X. Y.; Zhu, H. L.; Chen, Y. C.; Shang, Y. Y.; Cao, A. Y.; Hu, L. B.; Rubloff, G. W. MWCNT/V_2O_5 Core/Shell Sponge for High Areal Capacity and Power Density Li-Ion Cathodes. *ACS Nano* **2012**, *6*, 7948–7955.
17. Liu, B.; Zhang, J.; Wang, X. F.; Chen, G.; Chen, D.; Zhou, C. W.; Shen, G. Z. Hierarchical Three-Dimensional $ZnCo_2O_4$ Nanowire Arrays/Carbon Cloth Anodes for a Novel Class of High-Performance Flexible Lithium-Ion Batteries. *Nano Lett.* **2012**, *12*, 3005–3011.
18. Liu, B.; Wang, X. F.; Chen, H. T.; Wang, Z. R.; Chen, D.; Cheng, Y. B.; Zhou, C. W.; Shen, G. Z. Hierarchical Silicon Nanowires-Carbon Textiles Matrix as a Binder-Free Anode for High-Performance Advanced Lithium-Ion Batteries. *Sci. Rep.* **2013**, 3.
19. Cheng, Q.; Song, Z. M.; Ma, T.; Smith, B. B.; Tang, R.; Yu, H. Y.; Jiang, H. Q.; Chan, C. K. Folding Paper-Based Lithium-Ion Batteries for Higher Areal Energy Densities. *Nano Lett.* **2013**, *13*, 4969–4974.
20. Evanoff, K.; Benson, J.; Schauer, M.; Kovalenko, I.; Lashmore, D.; Ready, W. J.; Yushin, G. Ultra Strong Silicon-Coated Carbon Nanotube Nonwoven Fabric as a Multifunctional Lithium-Ion Battery Anode. *ACS Nano* **2012**, *6*, 9837–9845.
21. Fang, X.; Ding, N.; Feng, X. Y.; Lu, Y.; Chen, C. H. Study of $LiNi_{0.5}Mn_{1.5}O_4$ Synthesized *via* a Chloride-Ammonia Co-precipitation Method: Electrochemical Performance, Diffusion Coefficient and Capacity Loss Mechanism. *Electrochim. Acta* **2009**, *54*, 7471–7475.
22. Fang, X.; Lu, Y.; Ding, N.; Feng, X. Y.; Liu, C.; Chen, C. H. Electrochemical Properties of Nano- and Micro-Sized Li-$Ni_{0.5}Mn_{1.5}O_4$ Synthesized *via* Thermal Decomposition of a Ternary Eutectic Li-Ni-Mn Acetate. *Electrochim. Acta* **2010**, *55*, 832–837.
23. Feng, X. Y.; Shen, C.; Fang, X.; Chen, C. H. Synthesis of $LiNi_{0.5}Mn_{1.5}O_4$ by Solid-State Reaction with Improved Electrochemical Performance. *J. Alloys Compd.* **2011**, *509*, 3623–3626.
24. Liu, H.; Wu, Y. P.; Rahm, E.; Holze, R.; Wu, H. Q. Cathode Materials for Lithium Ion Batteries Prepared by Sol-Gel Methods. *J. Solid State Electrochem.* **2004**, *8*, 450–466.
25. Zhong, G. B.; Wang, Y. Y.; Zhang, Z. C.; Chen, C. H. Effects of Al Substitution for Ni and Mn on the Electrochemical Properties of $LiNi_{0.5}Mn_{1.5}O_4$. *Electrochim. Acta* **2011**, *56*, 6554–6561.
26. Kim, J. H.; Myung, S. T.; Sun, Y. K. Molten Salt Synthesis of $LiNi_{0.5}Mn_{1.5}O_4$ Spinel for 5 V Class Cathode Material of Li-Ion Secondary Battery. *Electrochim. Acta* **2004**, *49*, 219–227.
27. Liu, J.; Manthiram, A. Understanding the Improvement in the Electrochemical Properties of Surface Modified 5 V $LiMn_{1.42}Ni_{0.42}Co_{0.16}O_4$ Spinel Cathodes in Lithium-Ion Cells. *Chem. Mater.* **2009**, *21*, 1695–1707.
28. Delacourt, C.; Laffont, L.; Bouchet, R.; Wurm, C.; Leriche, J. B.; Morcrette, M.; Tarascon, J. M.; Masquelier, C. Toward Understanding of Electrical Limitations (Electronic, Ionic) in $LiMOO_4$ (M = Fe, Mn) Electrode Materials. *J. Electrochem. Soc.* **2005**, *152*, A913–A921.
29. http://pyrografproducts.com/Merchant5/merchant.mvc?Screen=cp_nanofiber.
30. Trionfi, A.; Wang, D. H.; Jacobs, J. D.; Tan, L. S.; Vaia, R. A.; Hsu, J. W. P. Direct Measurement of the Percolation Probability in Carbon Nanofiber-Polyimide Nanocomposites. *Phys. Rev. Lett.* **2009**, 102.
31. Sui, G.; Jana, S.; Zhong, W. H.; Fuqua, M. A.; Ulven, C. A. Dielectric Properties and Conductivity of Carbon Nanofiber/Semi-Crystalline Polymer Composites. *Acta Mater.* **2008**, *56*, 2381–2388.